Inorg. Chem. **2006**, *45*, 5953–5960

Efficient Energy Conversion in Photochromic Ruthenium DMSO Complexes

Aaron A. Rachford,[†] Jeffrey L. Petersen,[‡] and Jeffrey J. Rack*,[†]

Department of Chemistry and Biochemistry, Ohio University, Athens, Ohio 45701, and C. Eugene Bennett Department of Chemistry, West Virginia University, Morgantown, West Virginia 26506-6045

Received February 28, 2006

The photochromic compounds *trans*- and *cis*-[Ru(tpy)(Mepic)(dmso)](OSO_2CF_3) (**2** and **3**, respectively; tpy is 2,2′:6′,2″-terpyridine; Mepic is 6-methyl-2-pyridinecarboxylate; dmso is dimethyl sulfoxide) and *cis*-[Ru(tpy)(Brpic)(dmso)]-(PF_6) (**4**; Brpic is 6-bromo-2-pyridinecarboxylate) were prepared and characterized by single-crystal X-ray crystallography, electrochemistry, NMR, IR, and UV–vis spectroscopy. The geometry labels refer to the relationship between the carboxylate oxygen of the picolinate ligand and dmso. Electrochemical studies reveal that only the trans isomer shows S-to-O isomerization following oxidation of Ru(II) and O-to-S isomerization following reduction of Ru(III). The cis isomers of both complexes feature reversible one-electron Ru(III/II) couples. All complexes undergo phototriggered S-to-O isomerization following MLCT (metal-to-ligand charge transfer) excitation with quantum yields ($\Phi_{S\rightarrow O}$) of 0.79 (**2**), 0.011 (**3**), and 0.014 (**4**). The methyl group in **2** promotes isomerization by hindering rotation of the dmso ligand about the Ru–S bond. Computational results support this role for the methyl group. Relative energy calculations show that the barrier to rotation is approximately 8 kcal mol^{-1}. These results suggest that rotation is an important vibration for isomerization in photochromic ruthenium–dmso complexes.

Introduction

A critical feature of chromophores which act as photonic devices is the efficient conversion of photonic energy to potential energy. In photochromic compounds, potential energy is specifically required for bond formation or structural reorganization. As a result, molecular bistability and photonic triggering mechanisms for state transfer are essential for this field of study. Designing such molecules requires the incorporation of electronic structural features which promote proficient energy conversion in these processes.

In contrast to organic photochromic systems based on photocyclic ring-closing reactions,[1] coordination complexes featuring photoswitchable behavior are less common.[2,3] However, an exciting, new strategy to design such a class of molecules may be found in phototriggered linkage isomerization.[4] Here, a complex containing an ambidentate ligand bound to a central metal atom is excited with light to trigger linkage isomerization. This approach requires the development of transition metal complexes which feature this reactivity.

Our previous reports have highlighted electronic effects on the quantum yield of S → O isomerization in ruthenium and osmium polypyridine dimethyl sulfoxide (dmso) complexes (Chart 1).[5−9] For ruthenium complexes, ligands such as malonate (mal) and acetylacetonate (acac) inhibit formation of the corresponding O-bonded isomers.[5,6,8] Presumably, relatively low energy ligand field states shorten the excited state ^{3}CT (charge transfer) lifetime preventing isomerization. In contrast, ligands such as bipyridine (bpy) and 2-pyri-

* To whom correspondence should be addressed. E-mail: rack@helios.phy.ohiou.edu.
[†] Ohio University.
[‡] West Virginia University.

(1) Raymo, F. M.; Tomasulo, M. *Chem. Soc. Rev.* **2005**, *34*, 327−336.
(2) Gutlich, P.; Garcia, Y.; Woike, T. *Coord. Chem. Rev.* **2001**, *219*, 839−879.
(3) Sato, O. *Acc. Chem. Res.* **2003**, *36*, 692−700.
(4) Coppens, P.; Novozhilova, I.; Kovalevsky, A. *Chem. Rev.* **2002**, *102*, 861−883.
(5) Rack, J. J.; Winkler, J. R.; Gray, H. B. *J. Am. Chem. Soc.* **2001**, *123*, 2432−2433.
(6) Rack, J. J.; Mockus, N. V. *Inorg. Chem.* **2003**, *42*, 5792−5794.
(7) Rack, J. J.; Rachford, A. A.; Shelker, A. M. *Inorg. Chem.* **2003**, *42*, 7357−7359.
(8) Rachford, A. A.; Petersen, J. L.; Rack, J. J. *Inorg. Chem.* **2005**, *44*, 8065−8075.
(9) Mockus, N. V.; Petersen, J. L.; Rack, J. J. *Inorg. Chem.* **2006**, *45*, 8−10.

10.1021/ic0603398 CCC: $33.50
Published on Web 06/28/2006

Chart 1. Photoisomerizable Ruthenium-Polypyridine-dmso Compounds

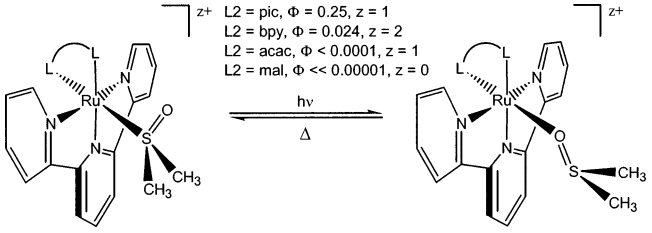

dinecarboxylate (pic) appear to enhance excited-state dmso isomerization. One intriguing attribute of these structural results was an apparent intramolecular C−H···O hydrogen bond between a C−H bond of the bidentate ligand and the oxygen of dmso.[8] We questioned the importance of this interaction and postulated that rotation about the Ru−S bond was an important vibration in excited-state S → O isomerization of dmso. Herein, we report the results of this study and propose that dmso rotation is a critical event in excited-state isomerizations of bound dmso.

Experimental Section

Materials. The complexes $Ru(tpy)Cl_3$, [Ru(tpy)(pic)Cl] and [Ru(tpy)(pic)(dmso)]PF_6 (**1**) were synthesized following literature procedures.[8,10,11] The ruthenium starting material ($RuCl_3 \cdot xH_2O$), silver trifluoromethanesulfonate (AgOTf), and silver hexafluorophosphate ($AgPF_6$) were purchased from Strem. The ligands, 2,2′:6′,2″-terpyridine (tpy), 2,2′-bipyridine (bpy), 2-pyridinecarboxylic acid (Hpic), 6-methyl-2-pyridinecarboxylic acid (Mepic), 6-Bromo-2-pyridinecarboxylic acid (Brpic), and dmso were purchased from Aldrich. Tetra(*n*-butylammonium) hexafluorophosphate ($TBAPF_6$) was purchased from Fluka and recrystallized from hot ethanol three times. Polymer (PMMA, poly(methyl methacrylate) Acros; PS, polystyrene, Aldrich, AMW 200 000) films containing the compounds for spectroscopic study were formed from room-temperature evaporation of acetonitrile/dichloromethane (7:3 v/v) solutions. Acetonitrile and dichloromethane for electrochemical experiments were of spectroscopic grade and purchased from Burdick and Jackson. All other reagents and solvents were used without further purification.

***trans*-[Ru(tpy)(Mepic)(dmso)](OTf) (2).** Dark purple [Ru(tpy)(Mepic)Cl] (172.1 mg, 0.32 mmol) was dissolved in 125 mL of 1,2-dichloroethane in the presence of excess dmso (500 μL) and 1 equiv of AgOTf (83.0 mg). The reaction mixture was refluxed overnight, under argon, and in the dark. The reaction mixture turned from purple to dark yellow-orange during this time. The solution was filtered hot to remove 1 equiv of solid AgCl. The filtrate volume was reduced to 3−4 mL, and the yellow-orange product precipitated with the addition of ethanol (5 mL) and ether (10−15 mL). The product was isolated by vacuum filtration, washed with ether (3 × 20 mL), and air-dried. Yield: 133.1 mg (58%). UV−vis (dmso) $\lambda_{max} = 428$ nm (5274 M^{-1} cm^{-1}). Emission (77 K) $\lambda_{em} = 593$, 667 nm. $E^{\circ\prime}$ $Ru^{3+/2+}$ vs Ag/AgCl = 1.31 (S-bonded), 0.61 V (O-bonded). ^1H NMR (CD_3CN): δ 8.45 (d, tpy), 8.41 (d, tpy), 8.25 (t, Mepic), 8.14 (t, tpy), 8.04 (m, tpy, Mepic), 7.85 (d, Mepic), 7.55 (t, tpy), 3.34 (s, $Mepic_{CH3}$), 2.39 (s, dmso). Anal. Calcd for $C_{25}H_{23}F_3N_4O_6RuS_2$: C, 43.03%; H, 3.33%; N, 8.03%; S, 9.20%. Found: C, 42.39%; H, 3.46%; N, 7.76%; S, 9.31%.

***cis*-[Ru(tpy)(Mepic)(dmso)](OTf) (3).** To the filtrate from the preparation of the trans material **2**, the cis product precipitated with the addition of ether as a microcrystalline solid. Yield: 12.5 mg. UV−vis (dmso) $\lambda_{max} = 447$ nm (5790 M^{-1} cm^{-1}). $E^{\circ\prime}$ $Ru^{3+/2+}$ vs Ag/AgCl = 1.07 (S-bonded), 0.72 V (O-bonded). ^1H NMR (CD_3CN): δ 8.42 (d, tpy), 8.39 (d, tpy), 8.34 (d, tpy), 8.10 (m, tpy, Mepic), 7.75 (t, Mepic), 7.61 (t, tpy), 7.05 (d, Mepic), 2.64 (s, $Mepic_{CH3}$), 2.51 (s, dmso). Anal. Calcd for $C_{25}H_{23}F_3N_4O_6RuS_2$: C, 43.03%; H, 3.33%; N, 8.03%; S, 9.20%. Found: C, 42.68%; H, 3.40%; N, 7.85%; S, 9.02%.

***cis*-[Ru(tpy)(Brpic)(dmso)](PF$_6$) (4). 4** was prepared following the procedure as described above for complex **2**. Yield: 65%. UV−vis (dmso) $\lambda_{max} = 440$ nm (3529 M^{-1} cm^{-1}). $E^{\circ\prime}$ $Ru^{3+/2+}$ vs Ag/AgCl = 1.11 (S-bonded), 0.74 V (O-bonded). ^1H NMR (CD_3CN): δ 8.43 (d, tpy), 8.39 (d, tpy), 8.27 (d, Brpic), 8.15 (t, tpy), 7.77 (t, Brpic), 7.64 (t, tpy), 7.44 (d, Brpic), 2.70 (s, dmso). Anal. Calcd for $C_{23}H_{20}BrF_6N_4O_3PRuS$: C, 36.42%; H, 2.66%; N, 7.38%; S, 4.23%. Found: C, 36.34%; H, 2.64%; N, 7.35%; S, 4.10%.

Instrumentation. Cyclic voltammetry was performed on a CH Instruments CH1730A electrochemical analyzer. This workstation contains a digital simulation package as part of the software package to operate the workstation (CHI version 2.06). The working electrode was a glassy-carbon or Pt electrode (BAS). The counter and reference electrodes were Pt wire and Ag/AgCl, respectively. Electrochemical measurements were typically performed in $C_4H_6O_3$ (propylene carbonate, PC) solutions containing 0.1 M $TBAPF_6$ electrolyte in a one-compartment cell. Electronic absorption spectra were collected on an Agilent 8453 spectrophotometer. Kinetic analyses of O → S rates determined in PC were performed on this same spectrometer. Goodness-of-fit for monoexponential plots was determined qualitatively by inspection of residual plots. Bulk photolysis experiments were conducted using a 100 W xenon-arc lamp (Oriel) fitted with a Canon standard camera UV filter. Infrared spectra were obtained on a Shimadzu Advantage FTIR-8400 spectrometer with KBr pellets. Proton nuclear magnetic resonance (^1H NMR) spectra were recorded on a 300 MHz Bruker AG spectrometer in deuterated acetonitrile (CD_3CN). Emission spectra were collected at 77 K in 4:1 ethanol/methanol on a PTI C-60 Fluorimeter equipped with a Hamamatsu R928 PMT (185−900 nm).

Crystallography. Crystals suitable for structural determination were obtained by slow evaporation of saturated acetonitrile/dmso solutions. Single crystals were washed with the perfluoropolyether PFO-XR75 (Lancaster) and sealed under nitrogen in a glass capillary. Samples were optically aligned on the four-circle of a Siemens P4 diffractometer equipped with a graphite monochromatic crystal, a Mo Kα radiation source ($\lambda = 0.71073$ Å), and a SMART CCD detector. The structure was drawn using ORTEP.

Quantum Yield of Isomerization. Quantum yields of isomerization were obtained by irradiating degassed solutions of $[Ru(tpy)(L2)(dmso)]^{z+}$ in PC at 298 K. Photolysis was achieved using a Continuum Nd:YAG laser pumped OPO (optical parametric oscillator) operating at 10 Hz. Incident radiation intensities were monitored by potassium ferrioxalate actinometry. A detailed explanation of the quantum yield procedure may be found elsewhere but is based on the procedure for determination of photosubstitution quantum yields.[8,12−16]

(10) Sullivan, B. P.; Calvert, J. M.; Meyer, T. J. *Inorg. Chem.* **1980**, *19*, 1404−1407.
(11) Dovletoglou, A.; Adeyemi, S. A.; Meyer, T. J. *Inorg. Chem.* **1996**, *35*, 4120−4127.
(12) Kirchhoff, J. R.; McMillin, D. R.; Marnot, P. A.; Sauvage, J.-P. *J. Am. Chem. Soc.* **1985**, *107*, 1138−1141.
(13) Suen, H.-F.; Wilson, S. W.; Pomerantz, M.; Walsh, J. L. *Inorg. Chem.* **1989**, *28*, 786−791.

Calculations. Low-level theory (PM3) calculations of the relative energies of each complex as a function of rotation angle (5°) about the Ru−S bond were performed by Spartan 02 on a Macintosh G4 machine. In this calculation, only the nonbonding interaction between the methyl groups of dmso and the 6-methyl-2-picolinate ligand was probed. No attempt was made to account for the electronic interactions of ruthenium with the bound ligands. The Ru−N and Ru−O bond lengths were constrained to values determined by the crystal structure. The Ru−S bond length was not constrained. Energy minimization predicts the correct orientation of the dmso ligand in the ground state as described by the crystal structure.

Results and Discussion

Synthesis and Structures. The new complexes prepared for this study are *trans*-[Ru(tpy)(Me-pic)(dmso)]$^+$ and *cis*-[Ru(tpy)(Me-pic)(dmso)]$^+$ (tpy is 2,2′:6′,2″-terpyridine; Me-pic is 6-methyl-2-pyridinecarboxylate), **2** and **3**, respectively, as well as *cis*-[Ru(tpy)(Br-pic)(dmso)]$^+$ (Br-pic is 6-bromo-2-pyridinecarboxylate), **4**. The geometry labels refer to the relationship between the carboxylate oxygen of the picolinate ligand and dmso. This geometry is identified by single-crystal X-ray crystallography and NMR spectroscopy. While **3** is isolated in small yield (∼10%) during the synthesis of **2**, *trans*-[Ru(tpy)(Br-pic)(dmso)]$^+$ was unable to be isolated, as the standard procedure routinely gave just **4**. In the standard procedure,[11] the bidentate ligand (Br-pic) is added to Ru(tpy)Cl_3 under reducing conditions to yield *cis*-[Ru(tpy)(Brpic)Cl] (the carboxylate oxygen is cis to Cl^-). Subsequent chloride abstraction with Ag^+ in the presence of dmso gives *cis*-[Ru(tpy)(Br-pic)dmso]$^+$. A simple explanation for this product distribution is the steric crowding at ruthenium caused by the orientation of Cl^- with Br in *trans*-[Ru(tpy)(Br-pic)Cl] (the carboxylate oxygen is trans to Cl^-), disfavors the formation of this product. Even in refluxing ethylene glycol for days, the trans product is not observed.

The structure of **2** is shown in Figure 1, with crystallographic data and selected metrical parameters displayed in Tables 1 and 2, respectively. The terpyridine ligand and bidentate 6-methylpicolinate ligands feature bond distances and angles similar to that of **1**.[8] The Ru−S and S−O bond distances are 2.2564(6) and 1.476(2) Å, respectively, and are within the accepted limits.[17,18] The Ru−S bond distance is slightly longer than that in [Ru(tpy)(pic)(dmso)]$^+$ (2.2152(5) Å). This lengthening of 0.041 Å is anticipated from the increased steric bulk of the methyl group in complex **2** relative to the hydrogen in the parent complex. Consistent with this change, the N4−Ru−S1 angle increases from 97.44(5)° to 106.43(6)° when Mepic is substituted for pic. The dihedral angle (N4−Ru−S1−O3), which represents dmso rotation about the Ru−S bond, changes from 51.7° to 57.4°. Increased rotation about this bond is expected due to the presence of the methyl group. Consistent with **1**, there appears to be a C−H···O_{dmso} interaction which serves to further orient the dmso ligand.[19] The C22···O3 distance is 3.066 Å and exhibits a C22−H22A−O3 angle of 139.34°. Importantly, large thermal displacement parameters are not observed within the dmso ligand. This suggests a single, low-energy configuration for this ligand and structure.

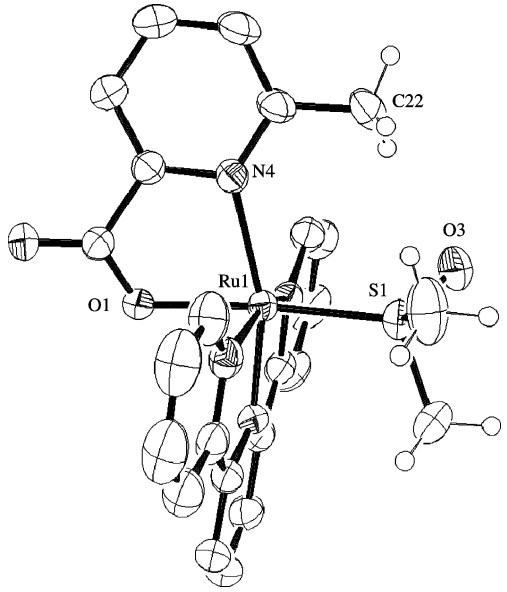

Figure 1. Perspective view of the molecular structure of *trans*-[Ru(tpy)(Mepic)(dmso)]$^+$ (**2**). Thermal ellipsoids are scaled to enclose 30% probability. Certain hydrogen atoms and labels have been omitted for clarity.

The cis geometry of the carboxylate group and the dmso ligand is seen in the structure of **3** (Figure 2). The Ru−N bond distances and angles for the coordinated terpyridine and picolinate ligands are unremarkable and are consistent with other structures.[20,21] The Ru−S and S−O bond distances are 2.241(1) and 1.471(4) Å, respectively, and are within the accepted range for S-bonded sulfoxides.[17,18] This Ru−S bond distance is slightly shorter than that of **2** and significantly shorter than that observed in [Ru(tpy)(bpy)(dmso)]$^{2+}$ (2.282(1) Å), a photoisomerizable Ru−dmso complex which features a nitrogen atom trans to dmso.[5] Unlike complexes **1** and **2**, the S═O bond of the sulfoxide is projected over the terpyridine ligand. This configuration of the sulfoxide was observed previously in the structures of [Ru(tpy)(acac)(dmso)]$^+$, [Ru(tpy)(mal)(dmso)], and [Ru(tpy)(ox)(dmso)] (ox is oxalate).[8] The C−H bonds from the methyl groups of dmso appear to be associated with the carboxylate oxygen of the Mepic ligand, as the C24···O1 distance is 2.997 Å with an angle of 112.3° (C24−H24B−O1).[19] Thermal displacement parameters indicate that the dmso ligand is not disordered and that only one conformation of this ligand is observed.

(14) Hecker, C. R.; Fanwick, P. E.; McMillin, D. R. *Inorg. Chem.* **1991**, *30*, 659−666.
(15) Bonnet, S.; Collin, J.-P.; Gruber, N.; Sauvage, J.-P.; Schofield, E. *J. Chem. Soc., Dalton Trans.* **2003**, 4654−4662.
(16) Murov, S. L. *Handbook of Photochemistry*; Marcel Dekker: New York, 1973.
(17) Calligaris, M.; Carugo, O. *Coord. Chem. Rev.* **1996**, *153*, 83−154.
(18) Calligaris, M. *Coord. Chem. Rev.* **2004**, *248*, 351−375.
(19) Desiraju, G. R. *Acc. Chem. Res.* **1991**, *24*, 290−296.
(20) Rasmussen, S. C.; Ronco, S. E.; Mlsna, D. A.; Billadeau, M. A.; Pennington, W. T.; Kolis, J. W.; Petersen, J. D. *Inorg. Chem.* **1995**, *34*, 821−829.
(21) Grover, N.; Gupta, N.; Singh, P.; Thorp, H. H. *Inorg. Chem.* **1992**, *31*, 2014−2020.

Table 1. Summary of Crystallographic Data for **2**, **3**, and **4**

L2 =	*trans*-Mepic	*cis*-Mepic	*cis*-Brpic
formula	$C_{25}H_{23}F_3N_4O_6RuS_2$	$C_{25}H_{23}F_3N_4O_6RuS_2$	$C_{23}H_{20}BrF_6N_4O_3PRuS$
fw	697.66	697.66	758.44
T, K	295(2)	295(2)	295(2)
space group	$P2_1/c$	$P2_1/n$	$P\bar{1}$
a, Å	12.8467(8)	9.298(1)	9.6184(5)
b, Å	8.7029(5)	16.491(2)	12.8578(7)
c, Å	24.2627(15)	18.014(2)	22.3180(12)
α	90°	90°	90.049(1)°
β	94.079(1)°	91.217(2)	92.051(1)°
γ	90°	90°	99.558(1)°
V, Å^3	2705.8(3)	2761.6(5)	2720.0(3)
Z	4	4	4
ρ_{calc}, g/cm^{-3}	1.713	1.678	1.852
total reflns	17 210	18 234	19 211
independent reflns	5989	6206	12 046
params	401	373	725
R1 (%)	5.30	5.57	4.72
wR2 (%)	14.27	13.79	12.20

Table 2. Selected Bond Distances and Angles for **2**, **3**, and **4**

L2	distance	(Å)	angles	(deg)
trans-Mepic	Ru−N1	2.084(2)	N1−Ru−N3	159.74(8)
	Ru−N2	1.954(2)	N1−Ru−N2	79.97(8)
	Ru−N3	2.075(2)	N2−Ru−N3	79.96(8)
	Ru−N4	2.197(2)	N1−Ru−S	93.48(6)
	Ru−O1	2.078(2)	N2−Ru−S	92.14(6)
	Ru−S	2.2564(6)	N3−Ru−S	89.97(5)
	S−O3	1.467(2)	N4−Ru−S	106.43(6)
	S−C23	1.782(4)	O1−Ru−S	175.12(5)
	S−C24	1.794(3)	O3−S−Ru−N4	57.4
cis-Mepic	Ru−N1	2.072(3)	N1−Ru−N3	159.3(1)
	Ru−N2	1.952(4)	N1−Ru−N2	79.7(1)
	Ru−N3	2.068(3)	N2−Ru−N3	79.8(1)
	Ru−N4	2.161(3)	N1−Ru−S	88.6(1)
	Ru−O1	2.087(3)	N2−Ru−S	88.8(1)
	Ru−S	2.241(1)	N3−Ru−S	93.7(1)
	S−O3	1.471(4)	N4−Ru−S	168.4(1)
	S−C23	1.772(5)	O1−Ru−S	89.9(1)
	S−C24	1.777(6)	O3−S−Ru−O1	149.9
cis-Brpic (*A*)	Ru1−N1	2.071(3)	N1−Ru1−N3	159.4(1)
	Ru1−N2	1.943(3)	N1−Ru1−N2	79.9(1)
	Ru1−N3	2.080(3)	N2−Ru1−N3	79.7(1)
	Ru1−N4	2.179(3)	N1−Ru1−S1	87.3(1)
	Ru1−O1	2.088(3)	N2−Ru1−S1	88.4(1)
	Ru1−S1	2.244(1)	N3−Ru1−S1	95.1(1)
	S1−O3	1.473(3)	N4−Ru1−S1	168.7(1)
	S1−C22	1.766(4)	O1−Ru1−S1	91.0(1)
	S1−C23	1.783(5)	O3−S1−Ru1−O1	136.5

Structural analysis of single crystals of **4** reveals two unique molecules in the unit cell (only one is depicted in Figure 3). These structures show a cis geometry between dmso and the carboxylate oxygen of the Br-pic ligand. The Ru1−S1 and Ru2−S2 bond distances of 2.244(1) and 2.240(1) Å, respectively, as well as the S1−O3 and S2−O6 bond distances of 1.473(3) and 1.472(3) Å, respectively, are similar to those observed in **3**. The two molecules in the unit cell are simple rotational isomers of one another. In one molecule, the dihedral angle formed from O1−Ru1−S1−O3 is 136.5°, whereas the corresponding angle (O4−Ru2−S2−O6) in the second molecule is 156.7°. The second molecule shows a greater rotation of the dmso ligand about the Ru−S bond. Similar to **3**, the S═O bond of dmso is projected over the terpyridine ligand. Short C−H···O_{Br-pic} contacts are also observed. Specifically, the distance for molecule 1 is 2.924 Å from C23···O1 with an angle of 97.76° (C23−H23B−O1), as well as 3.043 Å for C46···O4 in molecule 2 with an angle of 109.92° (C46−H46B−O4). These C−H···O interactions in **2**, **3**, and **4** are in the accepted range for C−H···O hydrogen bonds.[19]

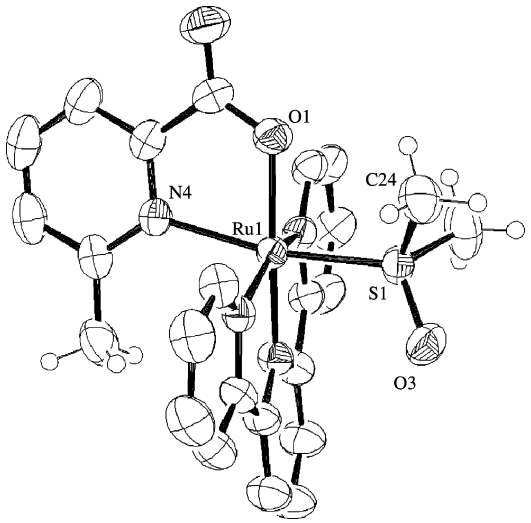

Figure 2. Perspective view of the molecular structure of *cis*-[Ru(tpy)(Mepic)(dmso)]$^+$ (**3**). Thermal ellipsoids are scaled to enclose 30% probability. Certain hydrogen atoms and labels have been omitted for clarity.

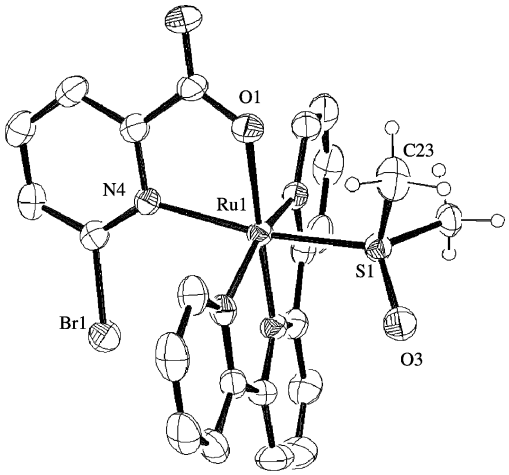

Figure 3. Perspective view of one of the unique cations of *cis*-[Ru(tpy)(Brpic)(dmso)]$^+$ (**4**). Thermal ellipsoids are scaled to enclose 30% probability. Certain hydrogen atoms and labels have been omitted for clarity.

Table 3. Spectroscopic and Electrochemical Data for Complexes **1**−**4**

	complex	λ_{max} S (nm)[a]	λ_{max} O (nm)[a]	$E^{\circ\prime}_S$ (V)[b]	$E^{\circ\prime}_O$ (V)[b]	$E^{\circ\prime}$(tpy/tpy$^-$) (V)[b]	$\phi_{S\rightarrow O}$	$k_{O\rightarrow S} \times 10^{-3}$ (s^{-1})
1	*trans*- [Ru(tpy)(pic)(dmso)]$^+$	419 (3.73)	518 (3.65)	1.31	0.57	−1.20	0.25 ± 1	1.0
2	*trans*-[Ru(tpy)(Mepic)(dmso)]$^+$	413 (3.72)	520 (3.64)	1.30	0.56	−1.19	0.79 ± 1	3.6
3	*cis*-[Ru(tpy)(Mepic)(dmso)]$^+$	447 (3.76)	506 (3.75)	1.07	0.72	−1.26	0.011 ± 2	0.37
4	*cis*-[Ru(tpy)(Brpic)(dmso)]$^+$	440 (3.55)	508 (3.57)	1.11	0.74	−1.26	0.014 ± 2	0.17

[a] Values in parentheses are log ϵ. [b] Values determined in 0.1 M $TBAPF_6$ propylene carbonate solution.

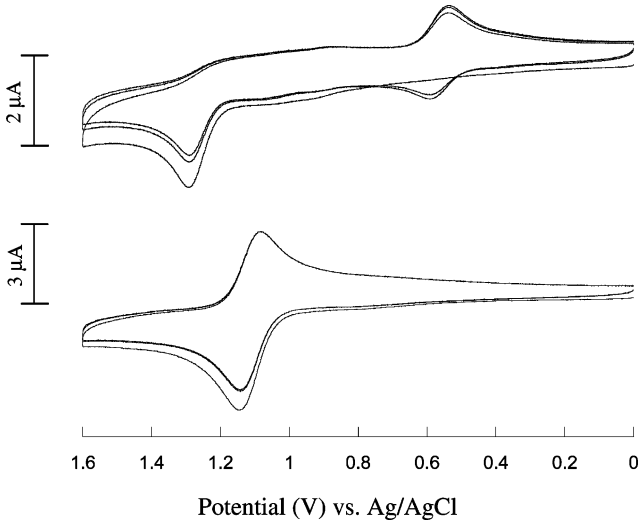

Figure 4. Voltammograms of *trans*-[Ru(tpy)(Mepic)(dmso)]$^+$ (**2**, top) and *cis*-[Ru(tpy)(Brpic)(dmso)]$^+$ (**4**, bottom); propylene carbonate solution, 0.1 M TBAH, glassy carbon working electrode, Pt counter electrode, Ag/AgCl reference electrode, $\nu = 0.1$ V s^{-1}.

Further evidence for intramolecular C−H···O interactions is observed by comparing the ^{1}H NMR spectra of complexes **2** and **3** (Supporting Information). It is expected that hydrogen bonding should result in downfield shifts due to decreased electron density around the proton. Comparison of δ_{Me} (Mepic) in **2** (3.34 ppm) and **3** (2.64 ppm) indicates a downfield shift of 0.7 ppm. Our interpretation of this dramatic shift is the presence of an attractive association between the 6-methyl group from Mepic and the oxygen from dmso in **2**. It seems unlikely that such shifts would be expected solely from cis−trans isomerism of the metal complex. Moreover, the methyl group (δ_{Me}) from dmso in **3** (2.51 ppm) is shifted downfield relative to that in **2** (2.39 ppm), indicating an interaction between this methyl group and the bound carboxylate oxygen of Mepic in **3**. Thus, the observed chemical shifts for the dmso protons and methyl group protons of the Mepic ligand are the confluence of three factors: the cis-trans geometry of the complex, the C−H interactions involving the sulfoxide in **2** and the carboxylate group in **3**, and the influence of the aromatic ring current provided by the proximity of the terpyridine ring.

Electrochemistry. The electrochemical data for these complexes are shown in Table 3. Representative cyclic voltammograms of **2** and **4** are shown in Figure 4. The top voltammogram reveals evidence of linkage isomerization following oxidation of S-bonded Ru^{2+} and reduction of O-bonded Ru^{3+}. Typical of complexes exhibiting this reactivity, voltammograms are consistent with an ECEC mechanism.[5,7,22−30] For **2**, the S-bonded $Ru^{3+/2+}$ couple is assigned to $E^{\circ\prime} = 1.30$ V (vs Ag/AgCl) and the O-bonded $Ru^{3+/2+}$ couple is assigned to 0.56 V in propylene carbonate solution. For comparison, the $Ru^{3+/2+}$ S-bonded and O-bonded couples for complex **1** are 1.31 and 0.57 V, respectively. Digital simulations of the voltammograms of **2** indicate the Ru^{3+} S → O isomerization rate is on the order of 50 s^{-1}, while the Ru^{2+} O → S is ∼2 × 10^{-3} s^{-1}, as seen in related complexes (Supporting Information).[8] This Ru^{2+} O → S rate matches well with the rate determined from bulk photolysis (see below).

Surprisingly, voltammograms of **4** (Figure 4, bottom) do not show evidence for isomerization following Ru^{2+} oxidation. A single one-electron couple is observed at 1.11 V vs Ag/AgCl and is assigned to the S-bonded $Ru^{3+/2+}$ couple. Similarly, a single one-electron $Ru^{3+/2+}$ couple is observed at 1.07 V for **3**. For both complexes, plots of I_p vs $\nu^{1/2}$ are linear and I_{pa}/I_{pc} ratios are unity, indicating reversible behavior under the scan rates investigated ($0.025 \le \nu \le 5$ V s^{-1}). Peak separations of 67 and 59 mV for **3** and **4**, respectively, are not suggestive of large molecular reorganization following electron transfer. The O-bonded couples of **3** and **4** were determined by bulk photolysis (see below) of electrochemical solutions containing these complexes. In this experiment, dilute solutions (∼0.1 mM) of **3** or **4** were irradiated in electrolyte solutions of propylene carbonate until full conversion had been achieved (15−60 min). Full conversion to the O-bonded isomers was evaluated from examination of the absorption spectra. These solutions were transferred to an electrochemical cell, and the standard cyclic voltammetry procedure was followed. The O-bonded couples were observed at 0.72 (**3**) and 0.74 V (**4**). It is interesting to note that the related complexes [Ru(tpy)(acac)-(dmso)]$^+$ and [Ru(tpy)(mal)(dmso)] do not show evidence of isomerization following electrochemical oxidation. Thus, complexes featuring a carboxylate oxygen cis to the sulfoxide ligand do not isomerize. Complexes featuring a trans carboxylate oxygen and an H or Me from the adjacent ligand (bpy, pic) within contact distance of the sulfoxide do isomerize.

(22) Nicholson, R. S.; Shain, I. *Anal. Chem.* **1964**, *36*, 706−723.
(23) Yeh, A.; Scott, N.; Taube, H. *Inorg. Chem.* **1982**, *21*, 2542−2545.
(24) Sano, M.; Taube, H. *Inorg. Chem.* **1994**, *33*, 705−709.
(25) Tomita, A.; Sano, M. *Inorg. Chem.* **1994**, *32*, 5825−5830.
(26) Tomita, A.; Sano, M. *Inorg. Chem.* **2000**, *39*, 200−205.
(27) Smith, M. K.; Gibson, J. A.; Young, C. G.; Broomhead, J. A.; Junk, P. C.; Keene, F. R. *Eur. J. Inorg. Chem.* **2000**, 1365−1370.
(28) Sano, M. *Struct. Bonding* **2001**, *99*, 117−139.
(29) Sens, C.; Rodriguez, M.; Romero, I.; Llobet, A.; Parella, T.; Sullivan, B. P.; Benet-Buchholz, J. *Inorg. Chem.* **2003**, *42*, 2040−2048.
(30) Johansson, O.; Lomoth, R. *Chem. Commun.* **2005**, 1578−1580.

The peculiar electrochemical results prompted a Lever-type analysis of these complexes.[31,32] Lever has shown that the observed $Ru^{3+/2+}$ reduction potential for a metal complex can be estimated from the sum of Lever parameters for each contributing ligand ($\sum E_L$). Most ligands are well-behaved within this model and such an analysis reveals details of metal−ligand bonding. In this analysis, a ligand is well-behaved if it exhibits a constant E_L value for a wide variety of ruthenium complexes. However, it has been shown that dmso is an electrochemically noninnocent ligand, meaning that the ligand does not give consistent and reliable E_L values for a series of ruthenium complexes. For example, the dmso ligand in $[Ru(tpy)(bpy)(dmso)]^{2+}$ exhibits an E_L of 0.64, whereas in $[Ru(tpy)(acac)(dmso)]^{+}$ the value is 0.58. Accordingly, our own analysis confirms this result regarding dmso and suggests a similar noninnocent behavior for the picolinate ligand. For example, cis−trans isomers of [Ru(tpy)(pic)Cl] (cis: $E^{\circ\prime} = 0.46$ V; trans: $E^{\circ\prime} = 0.39$ V) and $[Ru(tpy)(pic)(OH_2)]^{+}$ (cis: $E^{\circ\prime} = 0.38$ V; trans: $E^{\circ\prime} = 0.21$ V) feature substantial differences in their $Ru^{3+/2+}$ reduction potentials.[33] The variation in $E^{\circ\prime}$ as a function of geometry for these complexes is due to different stabilizing interactions between the pic and monodentate ligands in these sets of complexes. Typically, noncompliance with these ligand additivity rules is often suggestive of undetected synergistic bonding interactions within the complex. The variation in reduction potentials for complexes **1**−**4** and the electrochemical reactivity is likely due to undetected bonding interactions between picolinate and dmso.

Reversible ligand reductions are observed for complexes **1**−**4**. The terpyridine reduction appears in the range of −1.2 to −1.3 V vs Ag/AgCl, and the picolinate reduction appears in the range −1.7 to −1.9 V vs Ag/AgCl.[34] Interestingly, the L/L^- terpyridine reduction potential is insensitive to the donor atom of dmso in the metal complex. The identical tpy/tpy^- reduction potential is observed for both S- and O-bonded isomers within a single complex. This suggests that the MLCT excited states have energies that are nearly equal. Of course, the electrochemical experiment determines the ligand reduction on Ru^{2+} and not Ru^{3+}, whereas the excited states are characterized by a Ru^{3+} center.

Electronic Spectroscopy. The MLCT absorption maximum shifts from 413 nm in **2** to lower energy for the cis isomers **3** (447 nm) and **4** (440 nm), as suggested by the electrochemical data (Figure 5, Table 1). This is rationalized as the trans configuration features the π-donor carboxylate oxygen opposite that of the π-stabilizing dmso ligand. This synergistic interaction lowers the energy of the dπ set, resulting in a high-energy absorption maximum and a more positive $Ru^{3+/2+}$ couple. In contrast, the cis configuration results in two π-stabilizing ligands (pyridine and dmso) opposite one another, resulting in a lower-energy absorption maximum and a less-positive $Ru^{3+/2+}$ couple. It is this synergistic interaction that is not modeled well in the Lever analysis. The lowest-energy visible absorption in these spectra is primarily assigned to Ru d$\pi \rightarrow$ tpy π^* on the basis of energetic arguments. The picolinate one-electron reduction potentials are found at more negative potentials, which suggests that MLCT transitions involving this ligand would be found at higher energy.

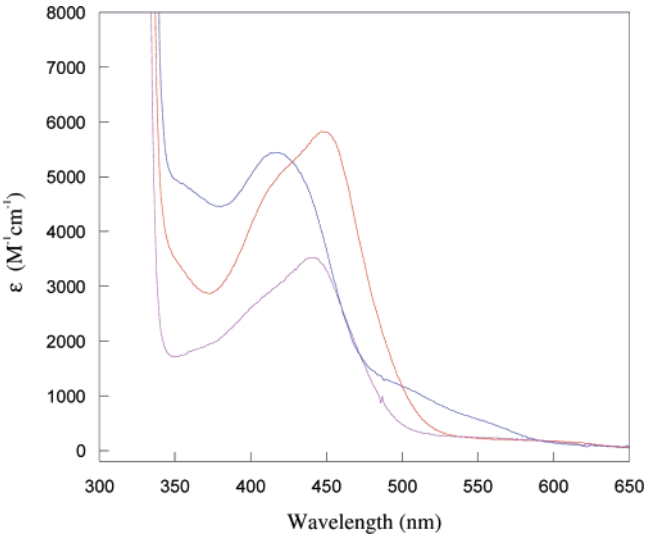

Figure 5. UV−vis absorption spectra of **2** (blue), **3** (red), and **4** (purple) in propylene carbonate.

The band shape and intensity of complexes **3** and **4** are typical of what is observed for many ruthenium polypyridine complexes.[34−36] The subtle features near 350 nm and the shoulder near 415 nm are likely due to higher-energy MLCT transitions and Ligand Field (LF) transitions.[37] The spectrum of **2** shows these features but also exhibits a relatively intense low-energy shoulder near 520 nm, shifted red of the main absorption feature at 413 nm. This feature in $[Ru(bpy)_3]^{2+}$ appears near 550 nm to the red of the main absorption at 452 and is assigned as direct ^{3}MLCT ← ^{1}MLCT excitation.[34] However, the intensities of the low-energy transitions are not comparable between the two complexes. For $[Ru(bpy)_3]^{2+}$, $\epsilon \approx 500\ M^{-1}\ cm^{-1}$ at 550 nm, whereas inspection of the spectrum of **2** reveals $\epsilon \approx 1200\ M^{-1}\ cm^{-1}$ at 520 nm. Given the unique photochemical reactivity of this compound (see below), it is tempting to suggest that this low-energy transition represents direct excitation to states which promote isomerization, as well as intensity associated with direct ^{3}MLCT excitation.

Excited-State DMSO Isomerization. Irradiation of **2**, **3**, or **4** in solutions or polymer films (PMMA or PS) results in dramatic changes in the electronic spectrum. The MLCT absorption maxima shift from 413 to 520 nm for **2**, from 447 to 506 nm for **3**, and from 440 to 508 nm for **4**. For

(31) Lever, A. B. P. *Inorg. Chem.* **1990**, *29*, 1271−1285.
(32) Lever, A. B. P.; Dodsworth, E. S. In *Inorganic Electronic Structure and Spectroscopy*; Solomon, E. I., Lever, A. B. P., Eds.; John Wiley and Sons: New York, 1999; Vol. II, pp 227−289.
(33) Llobet, A.; Doppelt, P.; Meyer, T. J. *Inorg. Chem.* **1988**, *27*, 514−520.
(34) Juris, A.; Balzani, V.; Barigelletti, F.; Campagna, S.; Belser, P.; Von Zelewsky, A. *Coord. Chem. Rev.* **1988**, *84*, 88−277.
(35) Felix, F.; Ferguson, J.; Gudel, H. U.; Ludi, A. *J. Am. Chem. Soc.* **1980**, *102*, 4096−4102.
(36) Kober, E. M.; Meyer, T. J. *Inorg. Chem.* **1982**, *21*, 3967−3977.
(37) Endicott, J. F.; Uddin, M. J. *Coord. Chem. Rev.* **2001**, *219*−*221*, 687−712.

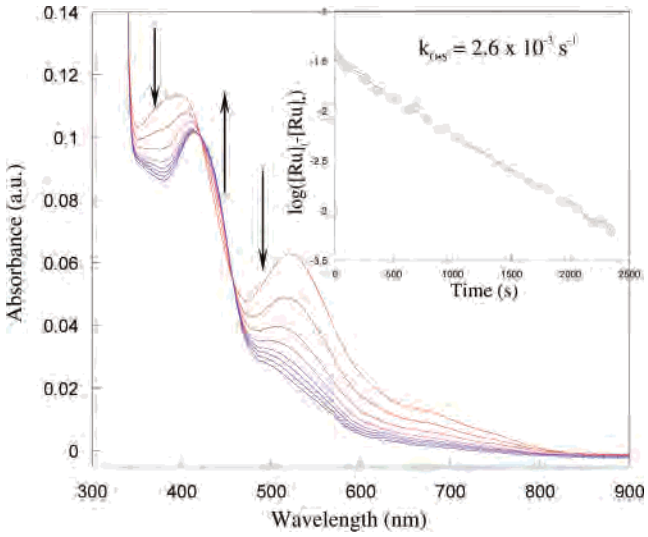

Figure 6. UV−vis absorption spectra of reversion of O-bonded [Ru(tpy)(Mepic)(dmso)]$^+$ (**2**) to S-bonded [Ru(tpy)(Mepic)(dmso)]$^+$ (**2**) in propylene carbonate. The inset shows the first-order plot of the reversion data (black) and the fit (red).

comparison, the S- and O-bonded absorption maxima for complex **1** are 419 and 518 nm, respectively. The energy difference between absorption maxima are similar for **1** (4570 cm^{-1}) and **2** (4980 cm^{-1}), as well as **3** (2610 cm^{-1}) and **4** (3040 cm^{-1}). These lower-energy absorption maxima mirror the electrochemical results and are consistent with O-bonded dmso. Reversion of the metastable O-bonded form to the ground-state S-bonded structure occurs at room temperature for all three complexes. Shown in Figure 6 are representative absorption spectra for complex **2** in propylene carbonate. The photogenerated O-bonded complex (red spectrum) thermally reverts to the ground-state S-bonded complex (blue spectrum). The plot of the kinetic trace at 520 nm (inset) follows first-order kinetics, as expected for an intramolecular isomerization.[6−8] In propylene carbonate solutions, the rates of O → S isomerization are 2.6(2) × 10^{-3} s^{-1} for **2**, 3.7(2) × 10^{-4} s^{-1} for **3**, and 1.7(3) × 10^{-4} s^{-1} for **4**. The thermal reversion rates in crystals and polymer films are much longer than in solution ($t_{1/2} \approx 1$ day). These rates are similar to the rates of isomerization that have been reported for other ruthenium polypyridine dmso complexes.[5−8,23−28]

Isomerization quantum yields ($\Phi_{S\rightarrow O}$) were determined for complexes **2**−**4** (Table 1). Most remarkable is the large $\Phi_{S\rightarrow O} = 0.79 \pm 0.01$ exhibited by complex **2**. Indeed, this compound is difficult to handle under standard fluorescent room lighting, as the reactivity is similar to that of the ferrioxalate actinometer. For complexes **3** and **4**, similar $\Phi_{S\rightarrow O} = 0.011 \pm 0.002$ and 0.014 ± 0.002, respectively, were determined. In comparison, complex **1** features $\Phi_{S\rightarrow O} = 0.25 \pm 0.001$, which is an order of magnitude increase relative to [Ru(tpy)(bpy)(dmso)]$^{2+}$ ($\Phi_{S\rightarrow O} = 0.024 \pm 0.001$).[8] The values for **3** and **4** are comparable to that of the bpy complex, which features a pyridine N donor atom trans to the sulfoxide. It is important to note that these complexes exhibit isomerization quantum yields that are at least an order of magnitude greater than the photosubstitution quantum yields that are typically observed in related ruthenium−terpyridine complexes.[12−14,38] Substituting pic for bpy represents an important change in the electronic structure with regard to isomerization. However, when Mepic is exchanged for pic, a greater than 3-fold increase in photoisomerization yield is observed. Given the similarity in the electronic structures of **1** and **2** (Table 3), this improvement in the isomerization quantum yield appears due to a nonbonding interaction between dmso and the methyl substituent of the Mepic ligand. Such an interaction suggests that rotation about the Ru−S bond is important for isomerization.

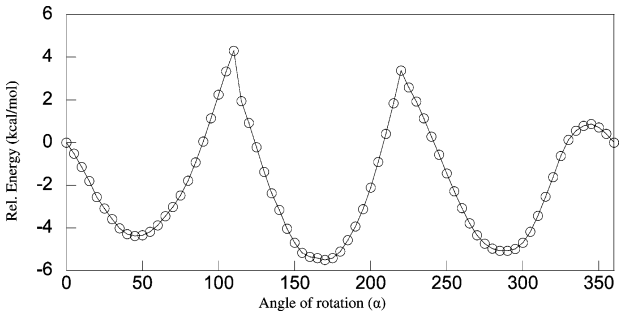

Figure 7. Plot of relative energy of *trans*-[Ru(tpy)(Mepic)(dmso)]$^+$ (**2**) vs dmso rotation angle about Ru−S bond.

Calculations. In an attempt to quantify the repulsive interaction between Mepic and dmso that results upon rotation of the dmso ligand, low-level theory (PM3) calculations were performed. In this calculation, no attempt is made to determine absolute energies or precise electronic structural information. Only the nonbonding spatial interaction between the methyl at the 6-position of Mepic and the methyl groups of dmso was interrogated. The relative energy of the complex as a function of rotation angle was determined. The relative energy is computed every 5° rotating the dmso ligand counterclockwise about the Ru−S bond. The arbitrary starting position coincides with a dihedral angle (N4−Ru−S−O1) of 0°, viewing down the Ru−S bond.

The structurally determined complex displays a dihedral angle of 57°, which is close to the first calculated minimum along the curve in Figure 7. Continued counterclockwise rotation of dmso about the Ru−S brings a methyl group from dmso in close contact with the methyl group from Mepic. This interaction is highly repulsive and is represented by the first sharp maximum near 110°. The second sharp peak near 220° corresponds with the second methyl group of dmso colliding with the Mepic ligand. The third lower-energy rounded peak corresponds to the oxygen atom of dmso passing near the methyl group during rotation. Continued rotation brings the dmso ligand back to its starting position.

One conclusion of these data is that the hydrogen atom of pic in **1** and the methyl group of Mepic in **2** serve to promote isomerization by disrupting rotation of dmso about the Ru−S bond. While the energy required to fully rotate the dmso ligand 360° is too large (∼8 kcal mol^{-1}) to occur in a complex at room temperature, the fact that a barrier to rotation is observed is important. The dmso need not rotate fully about the Ru−S bond, but rather only 20−30° is

(38) Bonnet, S.; Collin, J.-P.; Sauvage, J.-P.; Schofield, E. *Inorg. Chem.* **2004**, *43*, 8346−8354.

required to bring the methyl groups into near contact with the bidentate ligand. A rotation of this magnitude is possible within the excited-state lifetime of a molecule. Notably, phenyl rotations of 4,4′-diphenylbipyridine (dpb) in $[Ru(dpb)_3]^{2+}$ have been reported on a 2 ps time scale.[39] This action coupled with an already weakened excited state or oxidized Ru−S bond prompts isomerization. A similar barrier to rotation was determined from DFT calculations.[40]

Isomerization Mechanism. There are two obvious consequences from the geometry changes in cis and trans complexes listed in Table 3. First, dmso photoisomerizations in complexes in which the trans ligand is pyridine or a nitrogen donor atom exhibit relatively small quantum yields, whereas the yields are larger for a carboxylate oxygen donor atom. Previously, we suggested a dynamic interaction in which the *trans*-picolinate oxygen atom helps push the dmso away from the ruthenium, weakening the Ru−S bond and promoting isomerization.[8] The reduced photoisomerization quantum yield and absence of isomerization following electrochemical oxidation in the *cis*-picolinate complexes (**3** and **4**) serve to buttress this argument. A second consequence is the free rotation of the dmso ligand about the Ru−S bond. In the *cis*-picolinate complexes **3** and **4**, an obstruction to rotation is not evident. Thus, complexes **3** and **4** feature two characteristics that do not strongly promote photoisomerization.

The quantum yield data of **2** ($\Phi_{S\rightarrow O} = 0.79 \pm 0.001$) and computational data also suggest an important steric role for the ancillary ligands in the isomerization of dmso. One role for the methyl group is an excited-state mechanism in which rotation about the Ru−S bond occurs during or following formation of a thermally equilibrated charge transfer state. In this scenario, rotation about this bond brings the methyl groups of dmso in contact with the methyl group of Mepic in **2**. This conformation is repulsive, resulting in lengthening and eventual breaking of the Ru−S bond. The excited-state Ru^{3+}−S bond is characterized by weak, if nonexistent π-bonding, a situation that mitigates angular dependency on the bond strength. Another attractive proposal for the role of the methyl group in **2** is that it preselects ground-state geometries best suited for ^{3}CT isomerization. The increased dihedral angle, lengthened Ru−S bond distance, and oriented hydrogen bonds support this model. Both models allow for rapid LF deactivation of the CT states when the LF states are relatively low in energy, as in the examples of $[Ru(tpy)(acac)(dmso)]^+$ and [Ru(tpy)(mal)(dmso)] which do not show phototriggered isomerization. Given the structural data and the photochemical data, it is likely that both effects are operative.

(39) Damrauer, N. H.; McCusker, J. K. *J. Phys. Chem. A* **1999**, *103*, 8440−8446.
(40) Ciofini, I.; Daul, C. A.; Adamo, C. *J. Phys. Chem. A* **2003**, *107*, 11182−11190.

Conclusions

The large photoisomerization quantum yields for complexes **1**−**4** indicate that these complexes are able to access efficiently the energy stored in charge transfer states for bond forming reactions. It appears unlikely that photosubstitution and photoisomerization occur by similar mechanisms, given the disparity in the quantum yields for these two processes. Photosubstitution occurs by a LF-activated pathway in which population of these states labilizes the metal−ligand bond.[12−14] Photoisomerization occurs from a thermally equilibrated CT state and does not require population of LF states. Indeed, while photosubstitution does not occur in polypyridyl complexes of osmium,[12−14] we have recently observed dmso photoisomerization in $[Os(bpy)_2(dmso)_2]^{2+}$.[9] Further investigations to test the role of excited-state rotation and ground-state orientation of the sulfoxide are currently underway. In particular, direct measurement of isomerization rates and their temperature dependence will further our understanding of these complexes and their remarkable photoreactivity.

Acknowledgment. We thank Nicholas V. Mockus, Dennis Butcher, and Beth McClure for experimental assistance, as well as P. Greg van Patten and Michael P. Jensen for helpful discussions. PRF (38071-G3), Ohio University (1804 Fund), and the Condensed Matter Surface Science Program are acknowledged for financial support. A.A.R. thanks OU for an SEA award.

Supporting Information Available: ^{1}H NMR specta of **2**, **3**, and **4**; CIF files for **2**, **3**, and **4**; table of selected bond distances and angles for the second unique molecule of **4**; and representative digital simulations of voltammograms of **2**. This material is available free of charge via the Internet at http://pubs.acs.org.

IC0603398